Journal of Power Sources 193 (2009) 86–92

Contents lists available at ScienceDirect

Journal of Power Sources

journal homepage: www.elsevier.com/locate/jpowsour

Comparative study on the performance of pyrolyzed and plasma-treated iron(II) phthalocyanine-based catalysts for oxygen reduction in pH neutral electrolyte solutions

Falk Harnisch[a], Natalie A. Savastenko[b,*], Feng Zhao[a], Hartmut Steffen[b], Volker Brüser[b], Uwe Schröder[a]

[a] Institut für Chemie und Biochemie, Universität Greifswald, Felix-Hausdorff-Strasse 4, 17489 Greifswald, Germany
[b] Leibniz-Institute for Plasma Science and Technology, Felix-Hausdorff-Strasse 2, 17489 Greifswald, Germany

ARTICLE INFO

Article history:
Received 6 October 2008
Received in revised form 3 December 2008
Accepted 4 December 2008
Available online 24 December 2008

Keywords:
Microbial fuel cell
Oxygen reduction reaction (ORR)
Pyrolysis
Low-temperature plasma treatment
Iron phthalocyanine

ABSTRACT

The performance of pyrolyzed and plasma-treated non-precious catalysts for the oxygen reduction is discussed in the light of their application in microbial fuel cells. An Ar-radio frequency (RF) plasma treatment is applied to enhance the electrochemical activity of iron(II) phthalocyanine (FePc)-based catalysts. The electrochemical properties of the catalysts are analyzed by galvanodynamic linear sweep voltammetry and chronoamperometric experiments. Surface elemental analysis of the catalysts is examined by means of X-ray photoelectron spectroscopy (XPS). The influence of plasma power and treatment time on the elemental surface concentration and performance of the catalysts is investigated. The electrochemical activity, expressed in terms of the current density at 0 V vs. Ag/AgCl, is up to 40% higher for the plasma-treated samples than for pyrolyzed ones. It is found that optimal treatment time was 30 min and optimal plasma power was 150 W for the best electroactivity of FePc-based catalysts. From the results of XPS data, it is revealed that Ar-plasma treatment of the catalysts leads to an increase in the oxygen and nitrogen concentration on the catalysts surface. A correlation is found between the activity and surface concentration of oxygen and nitrogen on the catalysts' surface.

1. Introduction

Fuel cells and among these microbial fuel cells (MFCs) are promising technologies for a future sustainable electricity generation [1]. One common research interest is the development of catalysts for the cathodic oxygen reduction reaction (ORR) [2,3]. Desired qualities of electrocatalytic materials are e.g. low costs, high catalytic activity and high long time stability. Although platinum is considered to be the superior ORR electrocatalyst, its high – and further increasing – costs urge the search for non-noble-metal alternatives. Beside others, biomimetic electrocatalysts are a promising class of materials. Already in 1964 Jasinski [4] introduced transition metal-chelates as oxygen reduction electrocatalysts. Recently, several reviews have been published on the topic [5–7]. Iron (II) phthalocyanine was reported to be one of the most promising metal-chelates as catalysts for the oxygen reduction reaction under acidic conditions [8]. Recently it was also introduced as a cathode material for microbial fuel cells [9]. Despite the unique conditions (low ionic strength, pH neutral, ambient temperature) the principle performance of metal-chelate based catalysts showed similar trends for microbial and chemical fuel cells [2,9].

Despite a wealth of information on the ORR on iron phthalocyanine is available, e.g., on the influence of the carbon matrix on the catalyst performance [10,11], no practical applicability has yet been achieved. A lot of efforts have been made to improve these electrocatalysts. Soon after the proof of concept, it was found that a heat treatment under inert gas atmosphere (pyrolysis) can substantially improve the catalysts performance and long time stability [12]. Such heat treatment gives rise to modifications of macrocyclic structures with the appearance of interactions with the carbon support. Yet, in the process of catalysts treatment at high temperatures, unfavorable changes in morphology can occur, causing a detrimental decrease of the active surface [11]. This drawback can be overcome by using plasma treatment of the catalysts. Thus, it has been demonstrated that low-temperature plasma treatment is suitable to transform cobalt–tetramethoxymethylporphyrine (CoTMPP) into a catalytic material for the hydrogen peroxide and oxygen reduction reaction [13–15].

In this study, we applied an Ar-radio frequency (RF) plasma treatment to enhance the electrochemical activity of iron(II) phthalocyanine (FePc)-based catalysts. The plasma-treated and pyrolyzed FePc catalysts were compared in terms of

* Corresponding author. Tel.: +49 3834 554 413; fax: +49 3834 554 375.
E-mail addresses: savastenko@inp-greifswald.de, nataliesavastenko@tut.by (N.A. Savastenko).

0378-7753/$ – see front matter © 2008 Elsevier B.V. All rights reserved.
doi:10.1016/j.jpowsour.2008.12.049

their activity for the ORR and stability under typical MFCs conditions.

2. Experimental section

2.1. Reagents

Commercial (Sigma–Aldrich, Germany) iron(II) phthalocyanine (FePc, molecular formula $C_{32}H_{16}FeN_8$) was used as the precursor. Vulcan XC-72 (Cabot Corp.), beech graphite (Futurumshop) and technical graphite (Merck KGaA, Germany) were employed as catalyst support. High purity argon (99.999%, Air Liquid, Germany) was used for plasma treatment. The chemicals (KH_2PO_4, K_2HPO_4, H_3PO_4, KNO_3, HNO_3, tretrahydrofuran) were obtained from Sigma–Aldrich, Germany, Fluka, Germany and Merck KGaA, Germany. They were of analytical grade and used for electrolyte solution preparation without further purification. All electrolyte solutions were prepared using de-ionized water.

2.2. Preparation of catalysts

2.2.1. Pyrolysis

FePc was dissolved in tretrahydrofuran (THF) at room temperature, afterwards the mixture was added to a dispersion of 2 g of the carbon support (Vulcan XC-72, technical graphite powder and beech graphite) in THF, and was treated in an ultrasonic bath for 30 min. Subsequently, the THF was removed and the impregnated carbon material was heat treated under argon gas at 700 °C for 2 h. Finally, the material was ball-milled for 1 h. Additionally, a series of catalysts was prepared on oxidized carbon support. Therefore, Vulcan XC-72 was treated in 70% HNO_3 for 2 h under reflux, followed by thorough rinsing (until reaching pH neutrality) and drying in an oven at 80 °C.

2.2.2. Low-temperature plasma treatment

Plasma treatment was performed in inductively coupled radio frequency (RF) plasma generated in a vibrating bed reactor. The reactor illustrated in Fig. 1 is described in detail elsewhere [14]. Before each treatment, the reactor was evacuated to a pressure of 10^{-3} Pa. The experiments were carried out under gas flow conditions. The gas flow rate was 30 sccm. Pure argon was used at pressure of 10 Pa. The plasma power was varied in the range of 80–200 W. The plasma treatment time was varied from 5 to 90 min.

2.3. Electrode preparation

The cathode material was graphite foil (Chempur©, Karlsruhe, Germany). For galvanostatic half cell experiments graphite foils with an active surface area of 1 cm^2 were used. For electrode preparation, 1 mg of the respective catalyst material was manually distributed on the active surface area, using 10 μL of Nafion® solution (5%, Aldrich) as a binder. Then the electrode was allowed to dry at room temperature and was measured immediately.

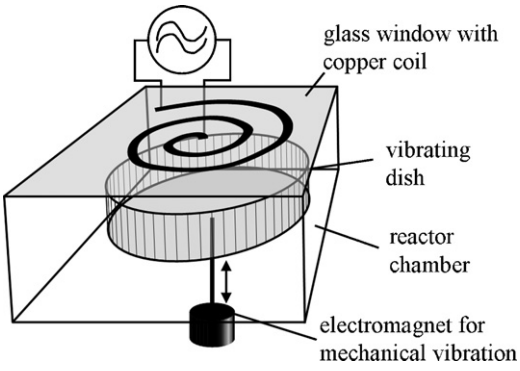

Fig. 1. Schematic configuration of a mechanically vibrating bed reactor.

2.4. Electrochemical characterization of catalysts

Galvanodynamic linear sweep voltammetry and chronoamperometry were carried out in a conventional three electrode arrangement using Autolab systems (PGSTAT 30, EcoChemie, Netherlands) interfaced to a personal computer. The reference electrode was a Ag/AgCl electrode (sat. KCl, Sensortechnik Meinsberg, Germany, 0.195 V vs. SHE). The experiments were carried out at room temperature. All catalyst performance data provided in this manuscript are based on galvanodynamic polarization experiments. From these experiments, which were performed at a scan rate of 10 μA s^{-1} (in continuously air purged electrolyte solutions) the respective current data were extracted as average values of forward and backward scan, for a potential of 0 V. The electrolyte solution was a 100 mM phosphate buffer adjusted either to pH 7 or pH 3.3. All potentials within this communication are given vs. Ag/AgCl (195 mV vs. SHE). All measurements were at least performed in three replicates and standard deviations were calculated to be below 5%.

2.5. Physical characterization of catalysts

X-ray photoelectron spectroscopy analysis (XPS) was used for the analyses of the samples after different treatments. XPS was performed on an Axis Ultra (Kratos, Manchester, UK). For the excitation of the photoelectron spectra Al Kα ($h\nu$ = 1.4867 keV) was used. Two sets of measurements were performed. From measurements with a pass energy of 80 eV the composition of the surface was estimated. Moreover high resolution measurements of the C 1s line with a pass energy of 10 eV were performed.

The elemental analysis was performed by the Industrial and Environmental Laboratory Vorpommern (Greifswald, Germany) according to the statutory procedure for carbon (DIN ISO 10694), nitrogen (DIN EN 25663) and iron (DIN EN ISO 11885). The BET specific surface area measurements were carried out using a Quantachrome Nova 2000 (Quantachrome, Inc.) surface area analyzer. Nitrogen gas was used as an adsorbate.

In situ mass spectrometry (MS) was applied for the characterization of the products during plasma treatment of catalysts. A mass spectrometer (Balzers QMG201) was directly connected to the plasma reactor.

3. Results and discussion

3.1. Choice of catalysts support

Since the selection of a suitable catalyst support is often essential for the catalyst performance we performed tests in order to choose the most suitable support material. For these tests, eight FePc-based catalysts with a loading of 50 wt% were prepared on different supports by the conventional pyrolysis and plasma treatment methods. Vulcan XC-72, HNO_3 treated Vulcan XC-72, beech graphite and technical graphite were used as catalysts supports. Ar-plasma treatment was carried out for 5 min at plasma power of 80 W. The differences among these catalysts in electrocatalytic activity for the ORR were characterized by means of galvanodynamic linear sweep voltammetry. Polarization results expressed as current densities at 0 V vs. Ag/AgCl are listed, together with the BET values of the respective support materials, in Table 1. Among all supports, Vulcan XC-72 had the highest specific surface area. Specific area lowered after HNO_3 treatment, which has already been reported by Shim et al. [16].

Table 1
Electrochemical performance of FePc-based catalysts using different supports. The current density at 0 V vs. Ag/AgCl was chosen as a measure of catalytic activity. The catalyst load was 5 wt%. Ar-plasma treatment was carried out for 5 min at plasma power of 80 W.

Different support	Preparation		BET ($m^2\,g^{-1}$)
	Pyrolysis j_0 ($mA\,cm^{-2}$)	Plasma treatment j_0 ($mA\,cm^{-2}$)	
Vulcan XC-72	−0.675	−0.765	220
HNO_3 treated Vulcan XC-72	−0.645	−0.775	133
Beech graphite	−0.475	−0.350	23
Technical graphite	−0.465	−0.400	120

As it can be seen from Table 1, Ar-plasma treatment induced different effects depending on the carbon support. A positive effect of the plasma treatment on the performance of catalysts – supported on both, treated and untreated, Vulcan XC-72 – is shown. Although the HNO_3 pretreatment of the support resulted in a decrease of the specific surface area, both pyrolyzed Vulcan-supported catalysts exhibited almost similar activity, and the Ar-plasma treatment led to a significant increase in the activity of both samples.

As it can be seen, the FePc-catalysts on beech graphite and technical graphite were less active than those supported on Vulcan XC-72, here a plasma treatment even reduced the ORR activity. Consequently, Vulcan XC-72 (untreated and HNO_3 treated) was chosen as catalysts support for further investigations.

3.2. Influence of plasma treatment on the electrochemical activity

Fig. 2 illustrates the dependence of the current density at 0 V (vs. Ag/AgCl) on the plasma power (P_{Plasma}) for catalysts supported on untreated and HNO_3 treated Vulcan XC-72. For comparison, data on plasma untreated (P_{Plasma} = 0 W) catalysts are also shown. As it can be seen, the effect of acid carbon pretreatment was observed only for the plasma-treated samples. For plasma untreated iron(II) phtalocyanine, no improvement of the performance was observed. For the catalysts treated in plasma, HNO_3 pretreatment of the carbon support led to a slight increase in activity (up to 12%) irrespective of plasma power. These results imply that oxidative acid pretreatment can promote the formation of catalytic centers, even though it reduces the specific surface area of the support. Fig. 2 also depicts the effect of the electrolyte pH on the performance of plasma-treated iron(II) phthalocyanine catalysts. As to be expected,

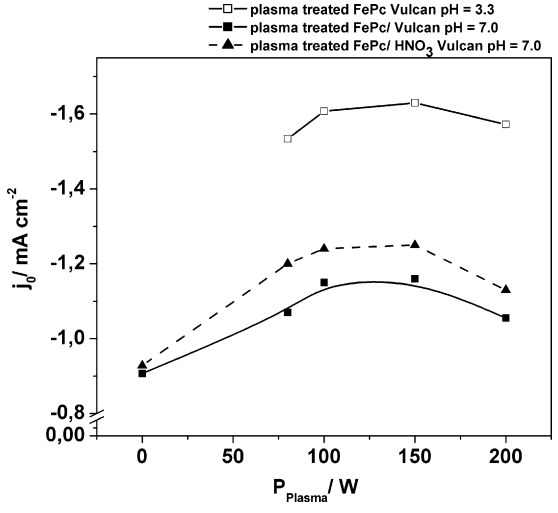

Fig. 2. Current density in 100 mM air saturated phosphate buffer solutions at pH 7 and pH 3.3 as function of plasma power at constant exposure time (5 min) for FePc – based catalysts. The catalyst load was 50 wt%.

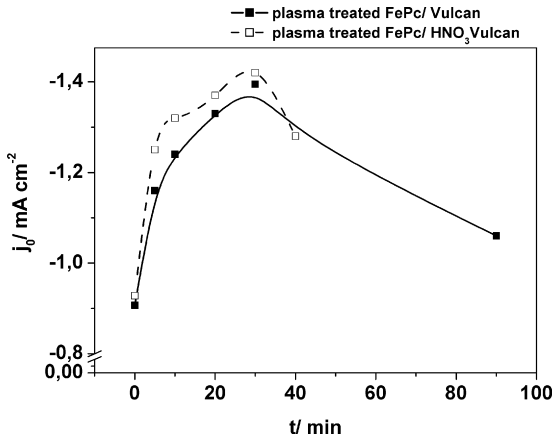

Fig. 3. Current density in 100 mM air saturated phosphate buffer solutions at pH 7 as a function of the plasma treatment time at constant power (150 W). The catalyst load was 50 wt%.

current densities are higher at acidic pH than at pH neutral conditions. A similar increase of the current density was reported in a previous work [2] and is mainly caused by the thermodynamic shift of the pH dependent redox potential of oxygen reduction reaction [17].

The results of Fig. 2 indicate the existence of optimal plasma treatment conditions. It appears that plasma treatment at low power (P_{Plasma} < 100 W) was not sufficient to convert the FePc-precursor. On the other hand, at high plasma power, a destruction of the catalytic centers seems to occur. The optimal plasma power was found to be 150 W; consequently all further treatments were performed using a plasma power of 150 W.

Fig. 3 shows the influence of the plasma treatment time on the catalyst activity at constant power. Clearly visible is a strong effect of the treatment time on the catalyst performance. The current density increases with increasing treatment time, to reach a maximum of about 1.4 $mA\,cm^{-2}$ (corresponding to an increase of the electrocatalytic activity of about 53% in comparison to the untreated material) at about 30 min treatment time. The current increase may be attributed to the increasing penetration depth of the plasma effect. After 30 min of treatment time further Ar-plasma treatment results in a decreasing catalyst activity, which may be explained by the decomposition of the formed catalytic centers.

Fig. 4 shows the electrocatalytic current densities plasma-treated and pyrolyzed samples as function of the catalyst load.

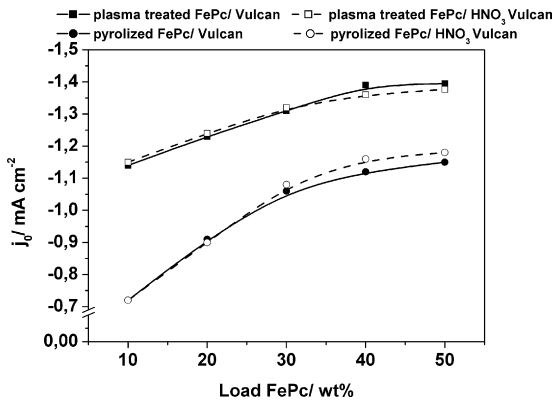

Fig. 4. Current density in 100 mM air saturated phosphate buffer solutions at pH 7 as a function of the relative catalyst load for heat treated and plasma-treated PcFe-based catalysts supported on untreated or HNO_3 treated Vulcan CX-72. Ar-plasma treatment was carried out for 30 min at plasma power of 150 W. The solution was stirred and permanently purged with air.

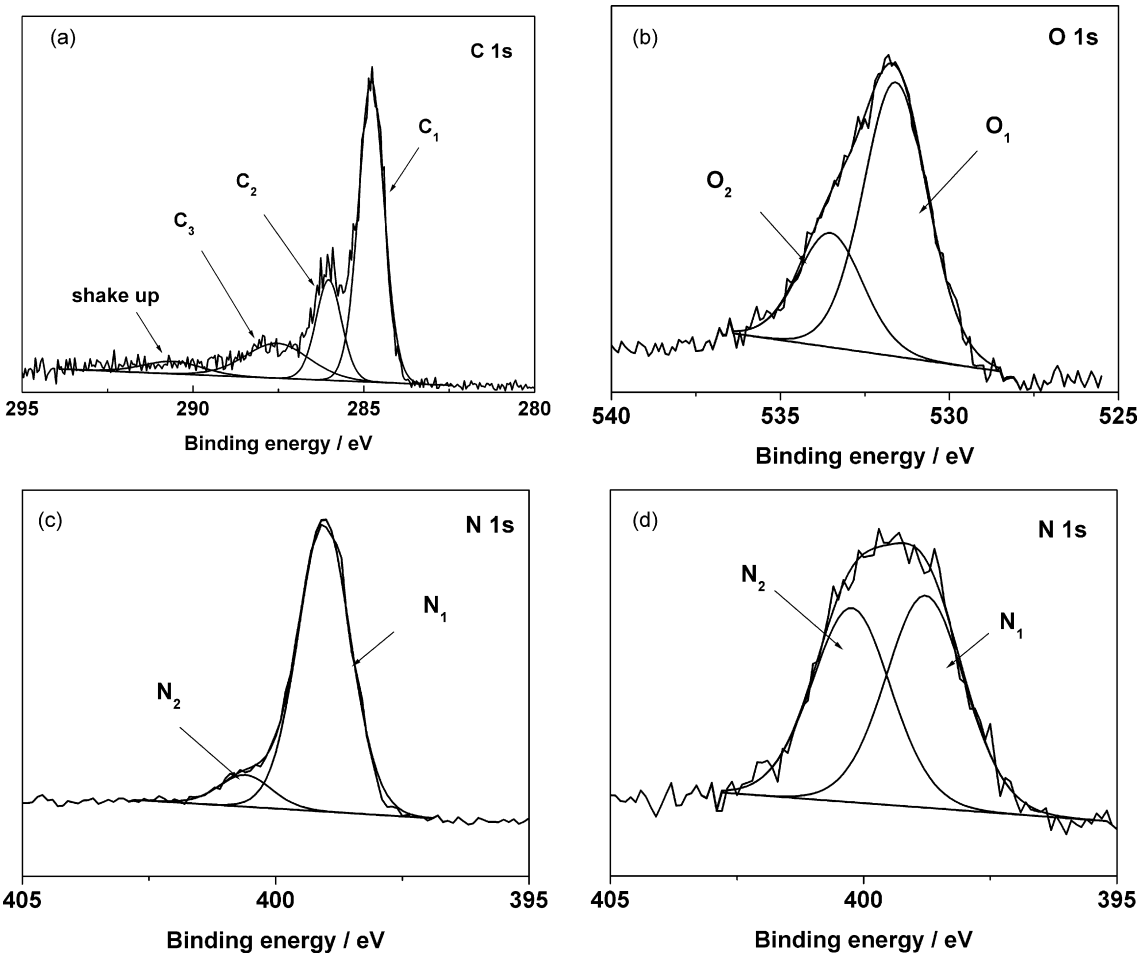

Fig. 5. Typical C 1s (a), O 1s (b) and N 1s (c and d) spectra of the untreated (a and c) and treated (b and d) samples.

Clearly visible is the superior catalytic activity of the plasma -treated samples compared to the pyrolyzed ones. The difference is more pronounced at low loading rates. For example, at 10 wt% FePc the plasma-treated material outperforms the pyrolysed one by about 40% (1.15 mA cm^{-2} vs. 0.72 mA cm^{-2}) whereas at higher loading rates, when both curves show a saturation behaviour, the difference is only ~20% (50 wt% FePc with 1.4 and 1.15 mA cm^{-2}, respectively). This effect may be attributed to electron transfer or mass transport limitation.

3.3. Long time stability

Long time stability experiments were carried out for pyrolysed and plasma-treated samples by continuous repeated galvanodynamic polarization between open circuit potential (OCP) and 0 V in air purged solutions, with a 30 min equilibration time between the consecutive cycles. No performance loss or catalyst degradation was observed after more than 150 cycles (more than 4 days).

3.4. Physical characterization of the catalysts

XPS and bulk elemental analyses were undertaken in order to explain the difference in catalytic behaviour of plasma-treated and pyrolyzed catalysts. XPS allows to evaluate the chemical change at the catalysts' surface as a consequence of the treatment. Generally, the difference in iron content on the surface of catalysts prepared by plasma treatment and pyrolysis can be neglected. The differences in oxygen and nitrogen surface concentration were more pronounced.

Fig. 5 shows the C 1s, O 1s, and N 1s regions of the typical XPS spectra. The spectra were fitted with elemental bands according to literature XPS functional group data [18–20]. The C 1s spectrum of Fe–Pc can be fitted with three elemental bands (peaks C_1–C_3 in Fig. 5a). The C 1s spectrum was fitted with a main band at 284.8 eV with full width at half maximum values (FWHM) of 0.8 eV. It is attributed to aromatic C—C bonds (graphitic carbons) [18]. This band comes from peripheral carbons of macrocycles [20]. The second component at 286.0 eV can be associated to N–C=N [20]. The 287.5 eV peak can be ascribed to carbon bound to oxygen by two oxygen bonds (C=O, N—C=O) [21]. A shake-up satellite appeared at 290.6 eV. For other samples, C 1s regions of spectrum consisted of one broad band at 284.8 eV (not shown). The peak deconvolution would be ambiguous. The shapes of the C 1s spectra were rather similar irrespective of the treatment procedure. The relative large FWHM value (3.2 eV) of the O 1s peak suggested the existence of two different oxygen species (Fig. 5b). The O 1s spectra were fitted with two peaks at 531.6 and 533.6 eV (peaks O_1 and O_2 correspondently). They can be attributed to oxygen atoms bonded to carbon atoms by double and by single bonds (C=O and C—O, respectively) [22]. The N 1s spectrum of FePc consisted of one main peak at 399.0 eV accompanied with a less intensive peak at 400.6 eV (Fig. 5c). The main peak (N_1) can be ascribed to the two chemically nonequivalent nitrogens (e.g. four central nitrogens and four aza nitrogens) [22]. They were not resolved because of XPS spectrometer resolution. A small energy separation between chemically different nitrogen atoms was also observed for CuPc, PtPc [19] and CuTPP [18,22]. The latter peak can be attributed to shake-up satellite [20,23,24]. For pyrolyzed and plasma-treated

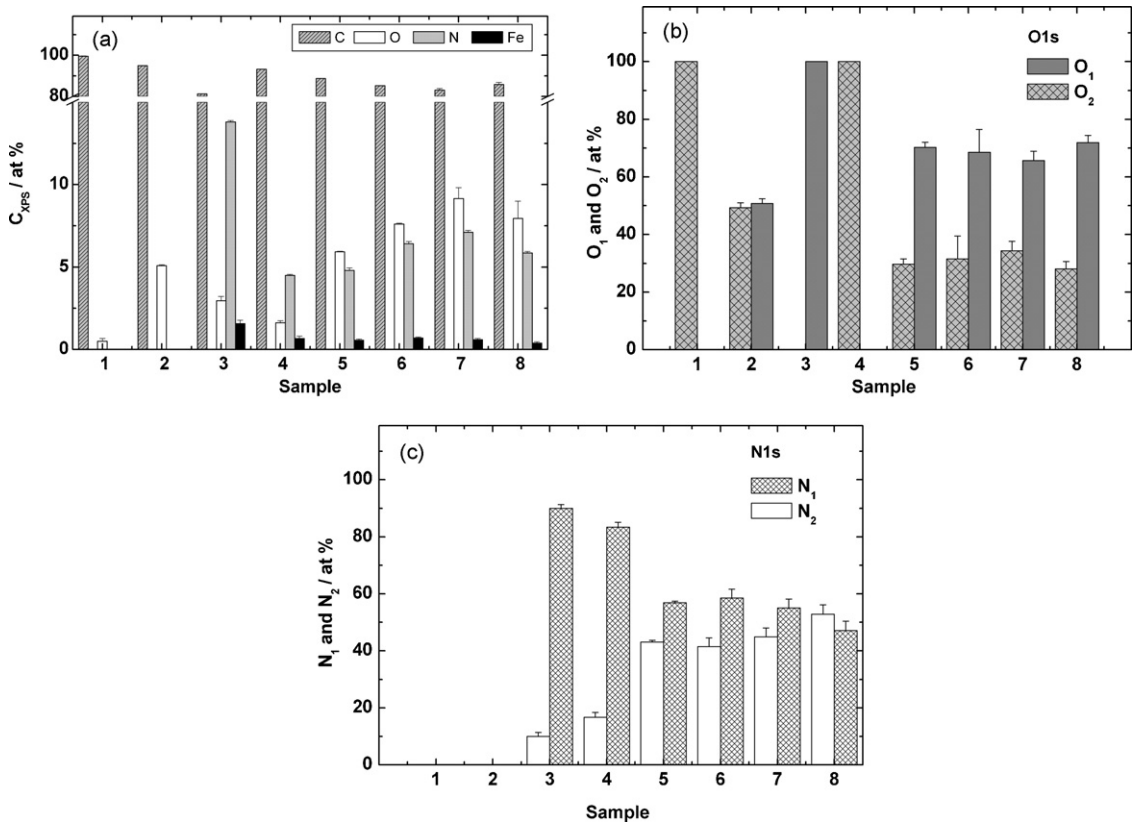

Fig. 6. The surface elemental concentrations of Fe, N, O and C (a), relative concentrations of O 1s (b) and N 1s (c) components on the catalyst after various steps of catalyst preparation: untreated Vulcan XC-72 (1); HNO_3 treated Vulcan XC-72 (2); unsupported catalyst precursor FePc (3); mixture of Vulcan XC-72 and precursor FePc (4); pyrolyzed FePc/Vulcan (5); FePc/Vulcan catalyst treated with plasma for 10 min (6), 30 min (7) and 90 min (8).

samples, an increase was observed in the XPS signal intensity at 400.6 eV. Fig. 5d shows the typical spectrum of treated sample. The shape of the N 1s spectra implied that new functional groups were formed on the samples' surface during heat or plasma treatment. For treated samples, it may be assumed that the shake-up satellite is overlapped with a new peak at around 400.6 eV. This new peak can be attributed to quaternary species (N-Q) or other nitrogen containing compounds (C═N─OH, O═C─N─C═O) [25,26].

Fig. 6 shows the N, O, C and Fe concentration on the catalysts surface after various steps of their preparation. Fig. 6a presents the atomic percentages of the various elements (C_{XPS}), as determined from the XPS signal. As XPS cannot detect hydrogen, the surface concentration of element C_j is expressed as:

$$C_{jXPS} = \frac{C_j}{C_{Fe} + C_N + C_C + C_O - C_H} \quad (1)$$

Fig. 6b and c depict the evolution of different oxygen and nitrogen species (relative component intensities O_1, O_2 and N_1, N_2 in at% of the total O 1s and N 1s peaks, respectively). The analysis of XPS data reveals that untreated FePc and catalysts support (samples 3 and 1, Fig. 6a and b) contained oxygen absorption impurities. Treatment of catalysts support with HNO_3 led to an increase in the oxygen surface concentration (sample 2, Fig. 6a). In addition, the oxygen-containing functionalities are transformed from O_2(C─O) to O_1(C═O) types of species (sample 2, Fig. 6b).

The pyrolysis resulted in an increase of the overall oxygen concentration and to a lower extent of the nitrogen concentration (samples 4 and 5, Fig. 6a). On the other hand, pyrolysis produced significant changes in the ratio of O_1/O_2 and N_1/N_2 components of oxygen- and nitrogen-containing functionalities, respectively. O_1 component of oxygen-containing functionalities was developed as a result of the pyrolysis (samples 4 and 5, Fig. 6b). After pyrolysis, an increase in the relative concentration of N_2 component was observed, while the concentration of N_1 species decreased. The increase in N_2 intensity suggests the formation of new types of nitrogen-containing functionalities.

The surface concentration of oxygen and nitrogen were first increased and then decreased with plasma treatment time (samples 6, 7 and 8, Fig. 6a). The maximal O and N surface concentrations were found on the surface of catalysts treated for 30 min. It should be stressed that catalysts treated for 30 min exhibited the highest activity. Exposure to the plasma induced an increase in the O_2 and decrease in O_1 components of oxygen – containing groups when the treatment time was less than 30 min (samples 6 and 7, Fig. 6a). With increasing plasma treatment time, the relative concentration of O_2 component decreased and O_1 component increased correspondently.

Several authors observed an increase in oxygen surface concentration after Ar-plasma treatment [5,27–29]. That fact might be explained by the oxidation of samples' surface by residual oxygen in the treatment chamber. On the other hand, a post-treatment effect may also contribute to the increased oxygen surface concentration. High energetic plasma species (Ar ions or electrons) interact with the surface of the sample breaking aromatic bonds and generating aliphatic fragments. Those fragments can promote the formation of oxygen-containing functionalities when the samples are exposed to the air after accomplishment of the plasma treatment.

An enrichment of the surface with nitrogen is without explanation yet. At present, it may be assumed that plasma treatment led to the decrease in surface concentration of C. The plasma can generate a reaction between carbon and water molecules adsorbed on

the surface of the sample. This reaction results in the formation of gaseous hydrogen and CO:

$$H_2O_{(ad)} + C_{(s)} \rightarrow CO_{(g)} + H_{2(g)} \quad (2)$$

The formation of carbon oxide and the presence of water vapour in the plasma reactor were further confirmed by mass spectrometry investigation.

Thus, reaction (2) leads to a lowering of the amount of carbon that can be detected by XPS. Decrease in C surface concentration means an increase in the ratios of N/C and O/C. Roughly speaking, the plasma treatment led to a "cleaning" of the catalyst surface from the carbon. As it can be seen from the Fig. 6a, that "cleaning" was successful when the treatment time did not exceeded 30 min. It might be assumed, that an increased treatment time led to further surface modification, and perhaps, destruction of FePc. That modification was unfavourable for both enrichment of surface with O and N and the catalytic activity of the samples.

According to the literature [27], the catalytic activity of Fe-based catalysts for the ORR depends on N content at the surface of catalysts support. The larger it is, the higher is the density of the catalytic sites and the better is the activity. Moreover, it was stated that the highest content of pyridinic-type nitrogen (binding energy 398.2 eV) is a determining factor for the catalytic activity [30]. It is supposed that there are two types of catalytic sites in the Fe-based catalysts. One of them is the central part of the macrocycles: FeN_4/C [27,31]. Another active site was denoted as FeN_2/C [27]. Villers et al. demonstrated that only pyridinic–type nitrogen is able to produce the FeN_2/C.

The correlation between enhanced electrocatalytic activity and a certain type of nitrogen containing species was not supported by our data. Firstly, no pyridinic-like nitrogen was detected. The N_1 peak (binding energy 399.0 eV) originated from nitrogens in FePc. The N_2 peak (binding energy 400.6 eV) can be associated either to the shake-up (for untreated FePc) or to the shake-up overlapped with peaks from other species (for treated samples). XPS indicated the changes in ratio of N_1- and N_2-type nitrogen after pyrolysis and plasma treatment (Fig. 6c). Nevertheless, the sample with the highest content of N_2-type of nitrogen did not coincide with the sample being the most active (Figs. 6 and 3 Figs. 6c and 3). Though, a clear correlation was found between the overall O and N content at the surface of the catalysts and their activity (Figs. 6 and 3 Figs. 6a and 3).

The elemental bulk analysis of the precursors and the pyrolysed respective plasma-treated samples revealed that the iron content (~5 wt%) was not affected by both preparation procedures whereas the pyrolysis diminished the nitrogen content from 9% to 4%, which was not influenced by the plasma treatment. It should be reminded here that both pyrolysis and plasma treatment increased the surface concentration of nitrogen and oxygen. This fact implies that pyrolysis led (among others) to a redistribution of nitrogen within sample. On the other hand, changes induced by the plasma treatment were too small to be observed with an elemental bulk analysis.

Roughly speaking, both bulk and surface concentrations of Fe remained almost constant irrelevant of the treatment procedure. Both plasma treatment and pyrolysis influenced the O and N surface concentration. Whereas the bulk composition of the catalyst may be affected only by pyrolysis. This difference is caused by the fact that plasma activated reactions take place only on the surface. They cannot significantly change the bulk properties of a catalyst. However, a change of species surface concentration likely has a substantial effect on the catalysts' performance.

3.5. Mass spectrometry of plasma during treatment of catalysts

In order to obtain more information regarding the processes involved in plasma treatment, *in situ* mass spectrometry (MS) analysis was performed. The plasma chamber was characterized at different stages: without Ar before turning on the plasma generator, with Ar without operating plasma sources as well as during plasma burning. The plasma reactor was loaded with FePc supported onto either untreated or HNO_3 treated Vulcan XC-72. The mass spectra were found to be independent either of support treatment or catalysts loading. Fig. 7a shows the typical mass spectra of the effluent gas before the plasma was generated and in the process of plasma treatment. The mass spectra were dominated by Ar^+, H_2O^+ and CO^+ (or N_2^+) ions. The peaks related to Ar appeared at $m/z = 40$ (Ar^+), 20 (Ar^{2+}) and 36 (Ar^+). The peaks related to O_2 (at $m/z = 32$ (O_2^+) and 16 (O^+)) and CO_2 (at $m/z = 44$ (CO_2^+)) were very weak. The MS peak at $m/z = 28$ can be attributed either to N_2 or CO. The appearance of MS signals at m/z of 28 and 30 in the ratio of N_2 and O_2 in air (4:1) would mean a leak in the reactor. Such ratio was not observed in mass spectra. It implies that MS signal at m/z of 28 was likely due to the CO formation. Fig. 7b depicts the intensity variation of peaks related to Ar^+, H_2O^+ and CO^+ (or N_2^+) vs. time. It can be seen that, once discharge was switched on, the MS signal at $m/z = 28$ increased. On the other hand, no changes were observed in the intensity of the MS signal related to water vapour after plasma was generated. That fact may be explained taking into account that the MS signal at $m/z = 28$ can be ascribed to CO. CO can be formed during plasma treatment of samples via reaction (2). Reaction (2) implies the consumption of water absorbed on the surface. Thus, it is not expected to change the amount of water vapour in the effluent gas.

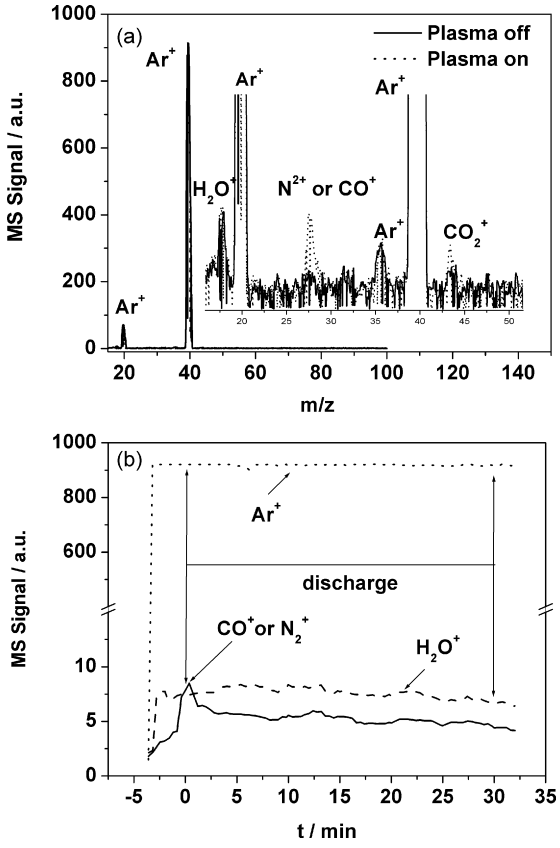

Fig. 7. Typical mass spectra in the process of plasma treatment of FePc-based catalyst (a). Data taken at discharge time from 0 to 1 min. Intensity variation of peaks related to CO^+ (N_2^+), H_2O^+ and Ar vs. time (b).

4. Conclusions

Our contribution shows the potential of a plasma treatment in the preparation of noble-metal-free electrocatalysts for the oxygen reduction reaction in microbial fuel cells. Under the conditions of

this study, the performance of plasma-treated FePc – based catalysts was superior to that of catalysts prepared by conventional pyrolysis method. The electrochemical activity under microbial fuel cell conditions, expressed in terms of the current density at 0 V vs. Ag/AgCl, was up to 40% higher for plasma-treated samples than that for pyrolyzed ones. It was found that the optimal plasma power was 150 W and optimal treatment time was 30 min. Oxidative pretreatment of catalyst support with HNO_3 seemed to enhance the catalytic activity through a promotion of the formation of catalytic centres while it decreased the catalysts specific surface area. It was found that Ar-plasma treatment of the catalysts led to an increase in the oxygen and nitrogen concentration on the catalysts surface. A correlation between O and N surface concentration and electroactivity of catalyst was observed.

Acknowledgements

F.H. greatfully acknowledges Ph.D. scholarships by the Deutsche Bundesstiftung Umwelt (DBU) and the Studienstiftung des Deutschen Volkes. U.S. acknowledges support by the Deutsche Forschungsgemeinschaft (DFG, Heisenberg program). U.S. additionally thanks the Fond der Chemischen Industrie (FCI). The authors are grateful to Dr. K. Schröder and Dr. A. Quade for fruitful discussion of XPS results.

References

[1] B.E. Logan, B. Hamelers, R. Rozendal, U. Schröder, J. Keller, S. Freguia, P. Aelterman, W. Verstraete, K. Rabaey, Environ. Sci. Technol. 40 (2006) 5181–5191.
[2] F. Zhao, F. Harnisch, U. Schröder, F. Scholz, P. Bogdanoff, I. Herrmann, Environ. Sci. Technol. 40 (2006) 5191–5199.
[3] Z. He, L.T. Angenent, Electroanalysis 18 (2006) 2009–2015.
[4] R. Jasinski, Nature 201 (1964) 1212–1213.
[5] C.W.B. Bezerra, L. Zhang, K.C. Lee, H.S. Liu, A.L.B. Marques, E.P. Marques, H.J. Wang, J.J. Zhang, Electrochim. Acta 53 (2008) 4937–4951.
[6] B. Wang, J. Power Sources 152 (2005) 1–15.
[7] S. Fukuzumi, H. Imahori, in: V. Balzani (Ed.), Electron Transfer in Chemistry, Vol. 2: Organic, Organometallic and Inorganic Molecules, Wiley-VCH, Weinheim, 2001, pp. 927–975.
[8] H. Jahnke, Ber. Bunsen-Ges. 72 (1968) 1053.
[9] F. Zhao, F. Harnisch, U. Schröder, F. Scholz, P. Bogdanoff, I. Herrmann, Electrochem. Commun. 7 (2005) 1405–1410.
[10] P. Vasudevan, Santosh, N. Mann, S. Tyagi, Trans. Metal. Chem. 15 (1990) 81–90.
[11] P. Bogdanoff, I. Herrmann, M. Hilgendorff, I. Dorbandt, S. Fiechter, H. Tributsch, J. New Mater. Electrochem. Syst. 7 (2004) 85–92.
[12] H. Jahnke, M. Schönborn, G. Zimmermann, Topics Curr. Chem. 61 (1976) 133–181.
[13] V. Brueser, N. Savastenko, A. Schmuhl, H. Junge, I. Herrmann, P. Bogdanoff, K. Schroeder, Plasma Processes Polymers 4 (2007) S94–S98.
[14] I. Herrmann, V. Bruser, S. Fiechter, H. Kersten, P. Bogdanoff, J. Electrochemic. Soc. 152 (2005) A2179–A2185.
[15] N.A. Savastenko, V. Bruser, M. Bruser, K. Anklam, S. Kutschera, H. Steffen, A. Schmuhl, J. Power Sources 165 (2007) 24–33.
[16] J.W. Shim, S.J. Park, S.K. Ryu, Carbon 39 (2001) 1635–1642.
[17] J.O.M. Bockris, U.M. Khan (Eds.), Surface Electrochemistry, A Molecular Level Approach, Plenum Press, New York, London, 1993, pp. 319–349.
[18] G.V. Ouedraogo, D. Benlian, L. Porte, J. Chem. Phys. 73 (1980) 642–647.
[19] Y. Niwa, H. Kobayash, T. Tsuchiya, J. Chem. Phys. 60 (1974) 799–807.
[20] G. Beamson, D. Briggs, High Resolution XPS of Organic Polymers: The Scienta ESCA300 Database, John Wiley & Sons, Chichester, 1992, pp. 277-282.
[21] R. Cueff, G. Baud, M. Benmalek, J.P. Besse, J.R. Butruille, M. Jacquet, Appl. Surf. Sci. 115 (1997) 292–298.
[22] H. Hochst, A. Goldmann, S. Hufner, H. Malter, Physica Status Solidi B-Basic Research 76 (1976) 559–568.
[23] J.L. Hueso, J.P. Espino's, A. Caballero, J. Cotrino, A.R. Gonza'lez-Elipe, Carbon 45 (2007) 89–96.
[24] P. Garcia, J.F. Espinal, C.S.M. de Lecea, F. Mondragon, Carbon 42 (2004) 1507–1515.
[25] Z. Tang, Q. Li, G. Lu, Carbon 45 (2007) 41–46.
[26] A. Felten, J. Ghijsen, J.J. Pireaux, R.L. Johnson, C.M. Whelan, D. Liang, G. Van Tendeloo, C. Bittencourt, J. Phys. D 40 (2007) 7379–7382.
[27] D. Villers, X. Jacques-Bedard, J.P. Dodelet, J. Electrochem. Soc. 151 (2004) A1507–A1515.
[28] F. Jaouen, S. Marcotte, J.P. Dodelet, G. Lindbergh, J. Phys. Chem. B 107 (2003) 1376–1386.
[29] J. Herranz, M. Lefevre, N. Larouche, B. Stansfield, J.-P. Dodelet, J. Phys. Chem. C 111 (2007) 19033–19042.
[30] J.A.R. Vanveen, H.A. Colijn, J.F. Vanbaar, Electrochim. Acta 33 (1988) 801–804.
[31] M. Lefevre, J.P. Dodelet, P. Bertrand, J. Phys. Chem. B 106 (2002) 8705–8713.